Aly *et al. Int J Concr Struct Mater (2024) 18:63*
https://doi.org/10.1186/s40069-024-00696-7

International Journal of Concrete Structures and Materials

RESEARCH Open Access

Development Length Assessment of Bonded Post-Tensioning Slabs with Bulb-Shaped Dead end Anchorage

Jehan H. Aly[1*], A. Farghal Maree[1], Mohamed Kohail[1] and Ayman H. Khalil[1]

Abstract

The bond between prestressing strands and concrete within the dead-end zone of a post-tensioned concrete member significantly influences the effectiveness of the strand-concrete system. However, the existing code equations for determining development length rely on studies conducted on pretensioned concrete members rather than post-tensioned ones. As a result, the implementation of development length for prestressing strands with bulb-shaped dead end anchorage in post-tensioning slabs relies on common practice and former experience. Unfortunately, this can sometimes lead to concrete cracks or strand slippage at the dead end zone due to insufficient development length. This paper presents an experimental study on post-tensioning slab segments representing the dead end zone. The aim of this study is to assess the development length of prestressing strands with bulb-shaped dead end that shall guarantee full bond with concrete throughout the member's service life. The Specimens were divided according to three different concrete compressive strengths 34 MPa, 48 MPa and 70 MPa. The parameters considered included slab thicknesses of 160 mm and 250 mm, as well as strand embedment lengths of 700 mm and 850 mm. Based on the test results, the sufficient development length was determined. Furthermore, a verification was carried out to assess the validity of applying predicted equations from an adopted bond model to determine the bond strength of strand with bulb-shaped dead end anchorage in concrete slabs.

Keywords Post-tensioning slabs, Development length, Bulb-shaped dead end anchorage

1 Introduction

Post tensioning system is a structural technique that is used in the construction of concrete slabs and other structural elements. It offers several advantages, as it allows for the best utilization of the concrete cross section by countering the dead load of the structural member with a prestressing force providing better crack and deflection control. Moreover, it enables longer spans to be achieved and minimizing the slab cross section needed (Mohammedali et al., 2021; Nawy, 2009).

Bonded post-tensioning system with embedded dead ends are commonly used in concrete slabs with longer spans as an efficient and economical structural solution. In the dead-end zone of the bonded post-tensioning slab a part of the strand is embedded directly into the concrete up to a certain length, while the remaining strand length is inserted into a flexible duct. Grout is then injected around the strand to ensure a monolithic behavior of the strand-concrete system. In a flexural member, the minimum bonded length required for reaching the nominal moment of the section is called "development length "(ACI, 2019). The development length (L_d) can also be defined as the minimum bonded length required to achieve the strand stress (f_{ps}) which is the stress

Journal information: ISSN 1976-0485 / eISSN 2234-1315.

*Correspondence:
Jehan H. Aly
g18023305@eng.asu.edu.eg
[1] Structural Engineering Department, Faculty of Engineering, Ain Shams University, Cairo, Egypt

experienced by the strand at the ultimate moment of a flexural member (ECP, 2018). The development length of strand with bulb-shaped dead end anchorage can be clearly illustrated as shown in Fig. 1.

Accurately assessing this length is essential to ensure a full bond between the concrete and the strand at the dead end zone without concrete cracks or deterioration during the tensioning process and throughout the service life of the member. The current development length equations presented in several codes are mainly based on experimental test results of pretensioned members (ACI, 2019; Hanson & Kaar, 1959). However there are differences between a pretensioned member and a post tensioned member concerning the time of strand tensioning, different bond mechanisms influencing the bond between the strand and the concrete, and the presence of various dead end types of prestressing strands used in post-tensioning systems.

Several types of strand dead ends are available in the market (Rogowsky & Marti, 1991), and each dead end exhibits its own bond behavior with concrete which influence the overall behavior of the strand–concrete system. The bulb-shaped dead end anchorage, also known in the construction market as H-anchorage dead end (Rogowsky & Marti, 1991; Aly et al., 2023) or onion dead end (Kobrosli et al., 2022), is one of the dead end types that can be easily shaped on-site in construction and is considered an economical fixed dead end (Rogowsky & Marti, 1991). The bond between concrete and strand at the dead end zone is a significant factor for successful strand-concrete behavior, depending on three main bond mechanisms: adhesion (Janney, 1954), mechanical interlocking resistance (Janney, 1954) and mechanical resistance of the bulb-shaped dead end anchorage (Rogowsky & Marti, 1991; Aly et al., 2023). The adhesion between 2 materials depends on the material's nature which vanishes at the first movement of any material relative to the other; therefore it has minimal effect on the bond behavior. Mechanical interlocking resistance arises from the concrete surrounding the helical shape of the strand, preventing twisting of the strand around its central axis during tensioning. The resistance of the bulb-shaped dead end also plays a significant role, as the concrete inside the bulb shape provides additional resistance against strand movement. The latter two bond mechanisms play vital roles in the bond behavior (Aly et al., 2023).

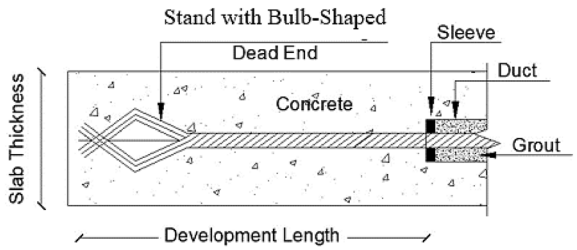

Fig. 1 Development length of post-tensioning slab with bulb-shaped dead end anchorage

The current implementation of development length for strands with bulb-shaped dead end anchorage depends on common practice values and former experience, which can lead to catastrophic slab failures during construction due to insufficient development length implemented with bulb-shaped dead end anchorage (Osama, 2009) or tensioning the strand in premature concrete. These reasons have prompted the need for this research.

In general there are several factors that affect the assessment of development length for strands in concrete (Mitchell et al., 1993; Fabris et al., 2018; Mohandoss et al., 2021; Mohandoss et al., 2020; Oh & Kim 2000; Dang et al., 2016; Dang et al., 2018; Martí-Vargas et al., 2013; Mohandoss et al., 2020b). One of the major factors is the concrete compressive strength because it mainly contributes to the bond (Mitchell et al., 1993; Fabris et al., 2018; Mohandoss et al., 2021; Mohandoss et al., 2020; Oh & Kim 2000; Dang et al., 2016; Dang et al., 2018; Martí-Vargas et al., 2013; Mohandoss et al., 2020b), along with the stress level in the prestressing stand (Mohandoss et al., 2021; Dang et al., 2016), concrete cover (Oh & Kim, 2000), strand spacing (Oh & Kim, 2000), and the strand diameter (Fabris et al., 2018a; Oh & Kim, 2000).

Several studies have been conducted to assess the development length of a free end strand in concrete (Dang et al., 2016; Dang et al., 2018; Martí-Vargas et al., 2013), (Transfer, Development, & Splice Length for Strand, Reinforcement in High-Strength Concrete, 2008; Jiang et al., 2019; Sorensen et al., 2019). Jiang (Jiang et al., 2019) conducted pull-out tests on 18 mm strand diameter with an ultimate strand strength of 1860 MPa, placed concentrically in concrete prisms with a cross section of 150 mm × 150 mm and a concrete compressive strength of 62.7 MPa. The study investigated different embedment lengths of 305 mm, 610 mm and 915 mm for a free end strand, recommending a safe development length of 915 mm. Sorensen (Sorensen et al., 2019) performed pull-out tests on 28.5 mm strand diameter placed concentrically in concrete prisms with a cross section of 200 mm × 200 mm and a concrete compressive strength of 55 MPa. The study concluded that specimens with an embedment length less than 1524 mm exhibited splitting failure, while 2438 mm was sufficient to reach the strand's ultimate strength. Additionally, Dang (Dang et al., 2018) conducted beam bending tests on specimens with a 15 mm diameter of tensioned strand to study the

effect of different concrete strengths on the development length assessment. It was concluded that using high strength concrete achieved a shorter development length than normal strength concrete.

2 Research Significance

The majority of the researches conducted on development length assessment have primarily focused on pretension members (Mitchell et al., 1993; Dang et al., 2016; Dang et al., 2018; Jiang et al., 2019; Ghosh & Fintel, 1986; Yang et al., 2018; Buckner, 1995; Dang et al., 2015; Naito et al., 2015; Logan 1997; Barnes et al., 1999; Dang et al., 2014; Fabris et al., 2018b). However, there has been relatively few studies conducted to study the development length in post-tensioning members or investigating the challenges associated with anchorages at dead end zones (Zghayar, 2007; Sofi et al., 2014). Due to the limited data concerning development length of post-tensioning members with bulb-shaped dead end anchorage, this experimental work was carried out. The aim of this research is to investigate the factors influencing the development length in post-tensioned slabs with bulb-shaped dead-end anchorage, thereby filling a gap in this research area and assessing a sufficient development length that ensure safety from the construction phase throughout the member's lifespan.

3 Experimental Work

In order to investigate the development length of strands with bulb-shaped dead end anchorage in post-tensioning concrete slabs, experimental tests were conducted on slab segments representing the dead end zone with different embedment lengths, slab thicknesses and concrete compressive strengths.

4 Material Properties

The constituents of the concrete mix were designed to achieve three different concrete compressive strengths after 28 days denoted by "N", "M" and "H". The concrete mixes "N" and "M" consisted of normal Portland cement, water, fine aggregates, coarse aggregates with maximum nominal size 20 mm. Mix "H" consisted of normal Portland cement, water, fine aggregates, coarse aggregates with maximum nominal size 10 mm and plasticizers to ensure better workability at lower water content. Standard concrete cubes were tested according to the ECP 203 (ECP, 2018) to evaluate the concrete compressive strength after 28 days. The average concrete compressive strengths were 34 MPa, 48 MPa and 70 MPa for mixes "N", "M" and "H" respectively. The concrete mix proportions for one cubic meter of concrete are as shown in Table 1.

In this experimental work, strands with 15.24 mm diameter (0.6 in), low-relaxation with cross section area equal to 140 mm^2 were used. The ultimate tensile strength of the strand was 1860 MPa, with a breaking force of 262 kN, and a modulus of elasticity of 195 GPa. The bulb-shaped dead end anchorage was shaped in the laboratory using a hydraulic jack. The anchorage had an average length of 120 mm, with the maximum width at the bulb part measuring approximately 65 mm. Also ordinary reinforced bars were used with 520 MPa ultimate strength and 360 MPa yield stress for both 10 mm and 12 mm steel diameters.

Table 1 Concrete mix proportions

Mix ID	Cement (kg)	Sand (kg)	Gravel (kg)	Water (kg)	Plasticizer (kg)
N	425	660	1025	235	–
M	425	660	1025	196	–
H	500	600	900	160	13.5

5 Specimen Dimensions

The experimental test consisted of 16 specimens, all with a rectangular cross-section and a constant width of 300 mm. This width was chosen to represent the spacing between strands in post-tensioning slabs and aligned with the maximum spacing listed in ECP 203 (ECP, 2018). The length of the specimens was chosen to be 750 mm and 900 mm. The 900 mm specimen length was selected to match the bonded length commonly implemented on-site, while the 750 mm length was chosen to investigate the feasibility of using shorter bonded length than what is typically implemented in post-tensioning slabs. The slab thickness varied between 160 and 250 mm.

6 Specimen Preparation and Reinforcement Details

Wooden forms were placed on a wooden deck for casting the slab segments. Inside the wooden form, a steel cage was placed and a strand was positioned at the middle height of the form. Steel chairs were used to keep all reinforcement in place. The reinforcement configuration was set up in each specimen to represent the reinforcement details of a dead end zone in a post-tensioning slab. The preparation of the specimens before concrete casting is shown in Fig. 2. Two longitudinal U shaped bars with 12 mm diameter were placed at both sides of the wooden form to represent the top and the bottom reinforcement of the slab segment. Additionally, four straight steel bars each with a diameter of 10 mm were tied with four stirrups also 10 mm in diameter around the bulb-shaped dead-end anchorage. The straight steel bars were placed in order to carry the tensile stresses

Fig. 2 Specimen's preparation before concrete casting

that may induce at the dead end location during loading, while the stirrups were used to confine the concrete around the bulb-shaped dead end anchorage. A concrete cover equal 25 mm was considered at the dead end side and 25 mm bond breaker was placed around the strand at the loaded side to prevent stress concentration. Thus, the clear bonded length (L_b) of the strand is equal the specimen length minus 50 mm. The reinforcement details of the specimens are illustrated in Fig. 3.

7 Specimens Configuration

The specimen's name was specified with 4 or 3 symbols. The first symbol denoted the concrete compressive strength (fc), with "N" representing 34 MPa, "M" representing 48 MPa, and "H" representing 70 MPa. The second symbol indicated the length of the specimen in cm, while the third symbol indicated the thickness of the specimen in cm. The fourth symbol, either "A" or "B" indicated the presence of two identical specimens. The configuration of specimens for all concrete mixes are as listed in Table 2.

8 Test Setup

To achieve the aim of this research an indirect pull-out test was used. This test method was suggested by previous studies (Aly et al., 2023; Farghal Maree & Hilal Riad, 2014). The test set up assembly consists of a horizontal fixed beam and a movable vertical steel column. The specimen was supported by the fixed horizontal beam, with the strand passing through a hole at its mid span. The strand was anchored at the top of the horizontal beam by using an anchor and wedge. The movable vertical steel column was equipped with top steel plates and holed bottom steel plates, facilitating the transfer of loads from the load cell to the specimen.

The test setup is considered as an indirect pull-out, where the strand remains fixed and compression force is applied on the concrete. Four Linear Variable Differential Transformers LVDTs were used to measure the strand slippage at the top side of the specimen. The test setup is as shown in Fig. 4.

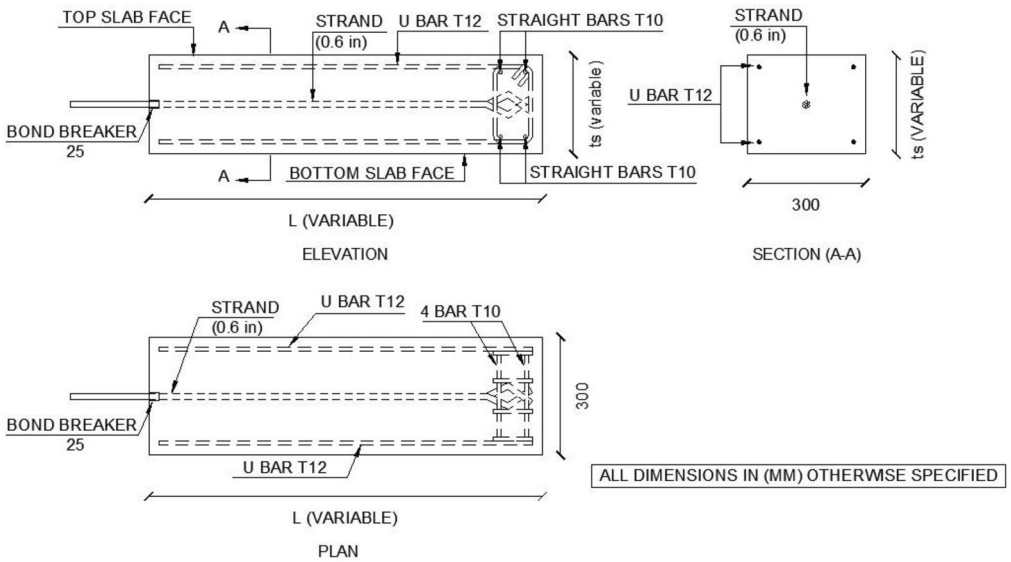

Fig. 3 Specimen's reinforcement details

Table 2 Specimen's configuration

Specimen name	Specimen width (mm)	Specimen length (L) (mm)	Bonded length (L_b) (mm)	Specimen thickness (ts) (mm)	f_c (MPa)
M-75-16-A	300	750	700	160	48
M-75-16-B					
M-75-25-A				250	
M-75-25-B					
N-90-16		900	850	160	34
M-90-16					48
M-90-25-A				250	
M-90-25-B					
H-75-16-A		750	700	160	70
H-75-16-B					
H-75-25-A				250	
H-75-25-B					
H-90-16-A		900	850	160	
H-90-16-B					
H-90-25-A				250	
H-90-25-B					

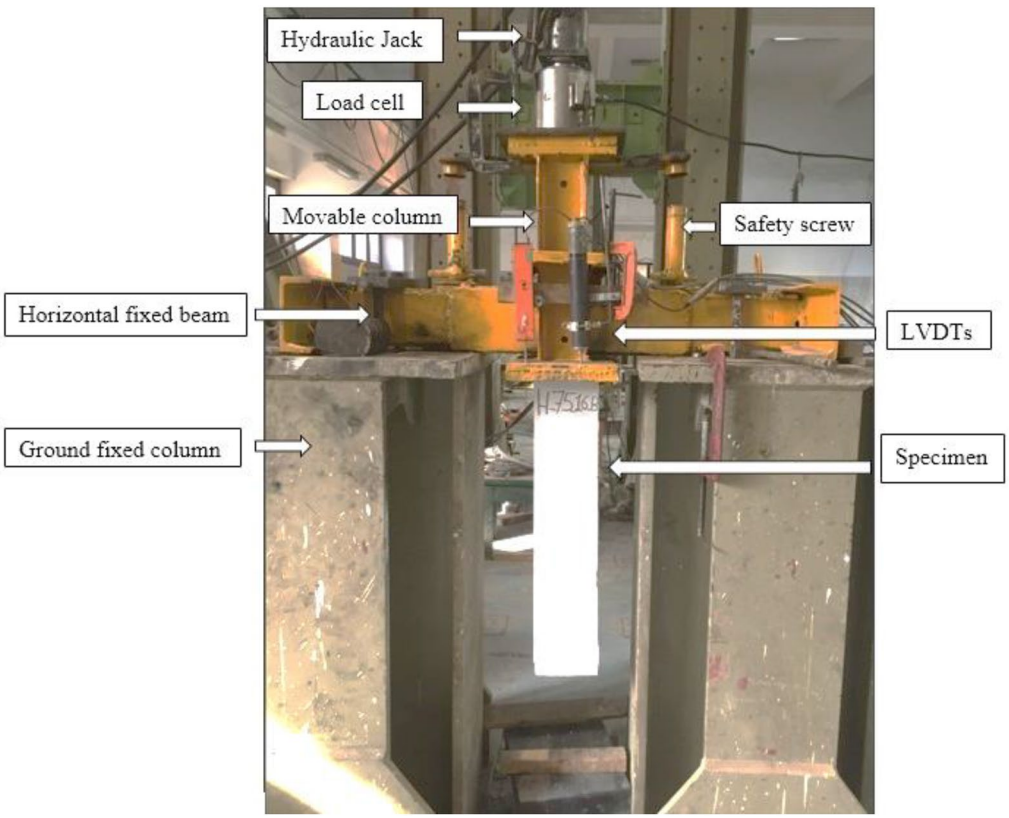

Fig. 4 Test set-up for indirect pull-out test

9 Test Results and Discussions

9.1 Ultimate Load and Maximum Stress

Table 3 summarizes the pull-out test results performed on the tested slab segments. The results include the ultimate load (P_u) and maximum strand stress (f_{pmax}). The f_{pmax} was compared with the initial prestressing stress (f_{pi}) which is the maximum stress allowed during the tensioning process before reduction of losses. The f_{pi} was considered according to ECP 203 (ECP, 2018) and ACI 318 (ACI, 2019) to be equal to 0.75 and 0.8 of the ultimate strand stress (f_{pu}), which are equal to 1395 MPa and 1488 MPa respectively.

All specimens with a length of 750 mm (700 mm bonded length) at f_c equal to 70 MPa and different slab thickness exceed the f_{pi} according to ECP 203 (ECP, 2018) and ACI 318 (ACI, 2019) in average 35% and 27% respectively. Similarly, specimens with the same bonded length with 48 MPa and a slab thickness of 250 mm exceed the f_{pi} according to ECP 203 (ECP, 2018) and ACI 318 (ACI, 2019) in average of 34% and 26% respectively. These specimens all achieved the expected strand breaking force.

However, specimens M-75-16-A and M-75-16-B with a slab thickness of 160 mm and f_c equal to 48 MPa did not reach the strand breaking force. They experienced several longitudinal and transverse crack propagation before failure. These specimens exceeded the f_{pi} according to ECP 203 (ECP, 2018) and ACI 318 (ACI, 2019) by an average 16% and 8% respectively.

It is worth noting that all specimens with a length of 900 mm (850 mm bonded length) and different concrete compressive strength (34 MPa, 48 MPa and 70 MPa) with varying slab thicknesses exceeded the f_{pi} according to ECP 203 (ECP, 2018) and ACI 318 (ACI, 2019) by an average of 35% and 27% respectively.They were all either near or reached the ultimate strand strength, as the longer bonded length allows for an excess force to shear off or crush the concrete surrounding the helical shaped part of the strand if compared with the shorter bonded length.

10 Crack Pattern and Failure Mode

By investigating the crack pattern of "M" specimens specified with concrete compressive strength equal to 48 MPa, it was observed that specimens with a length of 750 mm and a slab thickness of 160 mm were exposed to longitudinal cracks accompanied by transverse crack propagation at the dead end zone. This could be due to the presence of transverse tensile stresses that exceed the concrete's allowable tensile strength or due to the lower concrete confinement around the strand at a lower slab thickness. Increasing the slab thickness to 250 mm resulted in more concrete confinement around the bulb-shaped dead end anchorage leading to an obvious decrease in the crack propagation or almost complete disappearance of the cracks is shown in Fig. 5 for "M". Similar crack propagation was observed for specimens H-75-16-A and H-75-16-B, despite the concrete compressive strength being raised to 70 MPa. These specimens were exposed to longitudinal and transverse cracks, although they reached the strand's ultimate strength. In contrast, specimens H-75-25-A and

Table 3 Ultimate loads and maximum stress for the tested specimens

Specimen name	Ultimate strand load (Pu)	Maximum strand stress (f_{pmax})	f_{pmax}/f_{pi} (ECP) (2018)	f_{pmax}/f_{pi} (ACI)(2019)	Failure mode
M-75-16-A	228	1629	1.17	1.09	Concrete splitting
M-75-16-B	226	1614	1.16	1.08	Concrete splitting
M-75-25-A	261	1864	1.34	1.25	Strand failure
M-75-25-B	262	1871	1.34	1.26	Strand failure
N-90-16	259	1850	1.33	1.24	Concrete Splitting
M-90-16	272	1943	1.39	1.31	Strand failure
M-90-25-A	266	1900	1.36	1.28	Strand failure
M-90-25-B	263	1879	1.35	1.26	Strand failure
H-75-16-A	262	1871	1.34	1.26	Strand failure
H-75-16-B	263	1879	1.35	1.26	Strand failure
H-75-25-A	268	1914	1.37	1.29	Strand failure
H-75–25-B	263	1879	1.35	1.26	Strand failure
H-90-16-A	266	1900	1.36	1.28	Strand failure
H-90-16-B	262	1871	1.34	1.26	Strand failure
H-90-25-A	264	1886	1.35	1.27	Strand failure
H-90-25-B	260	1857	1.33	1.25	Strand failure

Fig. 5 Effect of increasing slab thickness on improving crack propagation in "M" specimens

Fig. 6 Effect of increasing slab thickness on improving crack propagation in "H" specimens

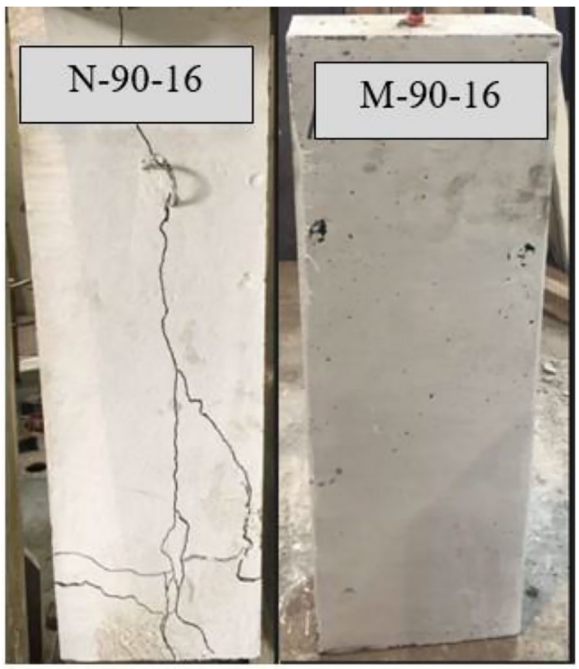

Fig. 7 Effect of concrete compressive strength on crack propagation

H-75-25-B, did not show any crack propagation before failure. This shows the positive effect of increasing the slab thickness in eliminating the concrete cracks. The crack pattern for "H" specimens is as shown in Fig. 6.

The impact of increasing the compressive strength of concrete on improving the allowable tensile strength of the concrete and reduction of cracks, can be clearly seen when comparing specimens M-75-25-B and H-75-25-A in Figs. 5, 6 respectively. This positive effect is also evident when comparing specimens N-90-16 and M-90-16, as shown in Fig. 7.

Although specimen "N" experienced intensive crack propagation both longitudinally and transversely, it reached an ultimate load of 259 kN, hich is close to the ultimate breaking force of the strand. This result demonstrates that a bonded length of 850 mm with fc equal to 34 MPa can ensure full bond with concrete. The same applies to all specimens of "M" and "H" mixes with bonded length of 850 mm, as they all reached the ultimate breaking force of the strand.

It is noteworthy that all "M" and "H" specimens, with a length of 900 mm and varying slab thicknesses, did not show any crack propagation before strand failure was observed.

11 Load—Displacement Relationships

Load versus strand displacement was recorded for all specimens up to failure. Two slippage values were subtracted from each strand displacement value recorded from the data acquisition device. The first value is the strand elongation for the unbonded strand located between the upper face of the specimen and the bottom anchor face. The second value is the wedge draw-in inside the anchor, which was evaluated from common practice and site experience to be equal 6 mm wedge draw-in at load of 190 kN. This draw-in value was estimated proportionally at every load increment until reaching 190 kN, and then fixed at a value of 6mm until reaching failure load.

The displacement values recorded included both the strand slippage and the elongation of the strand throughout the strand bonded length. The bulb-shaped dead end was considered a fixed anchoring point, so the elongation of the bulb-shaped dead end was not taken into consideration for simplicity. Energy absorption is the most observed feature from the load–displacement relationships. As the energy absorption is the process of dissipating the applied energy from external loading through plastic deformation or fracture (Yu & Xue, 2022). It is evaluated by the area under the curve in the load–displacement relation. As the area under the load–displacement relation increases, the specimen absorbs more energy and undergoes more plastic deformations until failure. For fc equal to 48 MPa, it was observed that specimens with a 250 mm slab thickness absorbed more energy until failure than specimens with a160 mm slab thickness for both 750 mm and 900 mm specimen lengths as shown in Fig. 8. Additionally, for the same concrete strength it was observed that specimens with 750 mm length showed some ductility performance due to the continuous propagation of cracks.

As shown in Fig. 9, specimens with fc equal to 70 MPa experienced approximately identical load–displacement performance for specimens with the same bonded length although they had different slab thicknesses. Also, the post peak behavior was characterized

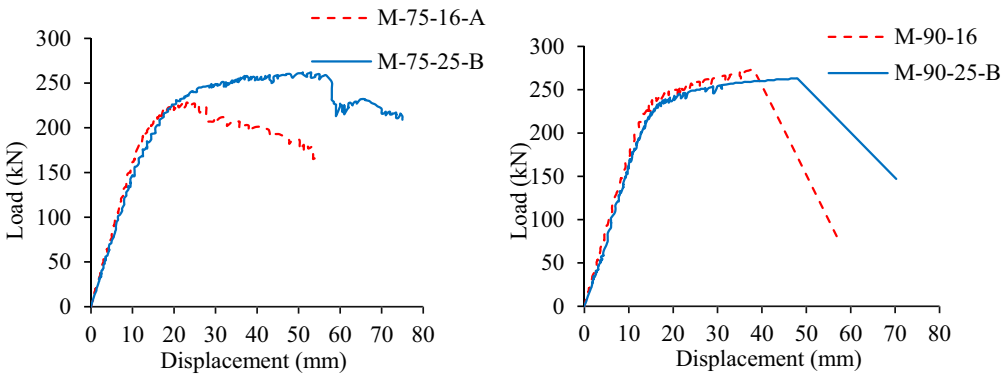

Fig. 8 Load–displacement relationships for "N" and "M" specimens

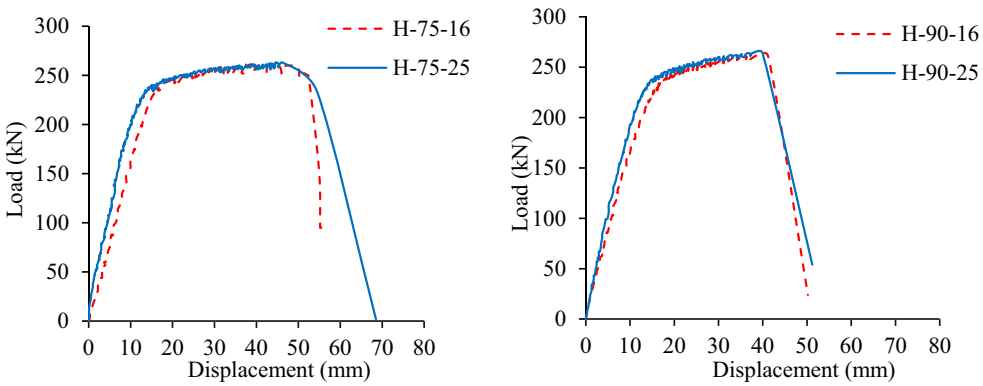

Fig. 9 Load–displacement relationships for "H" specimens

by sudden failure because the bonded length was sufficient for developing the strand ultimate strength.

12 Bond Model Background

Several bond models were predicted in order to understand the different bond mechanisms that influence the bond behavior between reinforced bars and concrete (Farghal Maree & Hilal Riad, 2014; Hong & Park, 2012; Hong et al., 2012; Tang, 2017; Tang, 2015; Lin et al., 2019; Mazumder et al., 2021; Tang & Cheng, 2020). Most of the bond models predicted previously refer to the bond model presented by the FIB Model code 2010 (Fédération Internationale du Béton, FIB Model Code & International Federation for Structural Concrete, 2013) which simulate the local bond stress-slip relationship between rebar and concrete as a basic assumption for their proposed bond models. The bond between concrete and strand was also studied by several researchers (Mohandoss et al., 2021; Martí-Vargas et al., 2013; Dang et al., 2014b; Peterman, 2009; Wang et al., 2022; Salmons and McCrate 1977; Shin et al., 2018). These studies demonstrated the different bond mechanisms that influence the bond between the straight strand and concrete. Some of these researches predicted bond models to express the bond behavior (Wang et al., 2022; Yang et al., 2022; Lee et al., 2017; Yi et al., 2020a; Wang et al., 2017; Dang et al., 2015b; Kareem et al., 2020). The available acceptance criteria for the bond between strand and concrete is standardized in the American Society for Testing Materials ASTM A1081 (ASTM 2015).It is determined by a pull-out test of a free end strand embedded concentrically in a cylindrical concrete specimen and evaluating the pullout force corresponding to a free end slip equal to 0.1 in. (2.5 mm). Jehan (Aly et al., 2023) predicted a bond model to simulate the bond between concrete and strand with bulb-shaped dead end anchorage, this bond model was adopted in this research as it is the available bond model in literature to express the bond behavior between concrete and strand with bulb-shaped dead end anchorage. The aforementioned bond model was based on experimental pull-out tests of 150 mm diameter cylindrical concrete specimens, with different specimen lengths 350 mm, 550 mm and 750 mm. Each specimen contains one concentric strand with bulb-shaped dead end anchorage. These specimens were tested under indirect pull-out test until failure. The adopted bond model refers to the bond model presented in the FIB Model code (CEB-FIP, 1990) between the rebar and the concrete as a base assumption in conducting their model. Some modifications took place in order to consider the differences between the rebar and the strand geometry which results in different bond mechanisms between each of them with concrete. An evaluation of the bulb-shaped anchorage capacity was also presented in this adopted model.

The adopted bond model (Aly et al., 2023) is characterized by four main stages as illustrated in Fig. 10 and expressed in Eqs. (1) and (2) respectively. The first stage is characterized by an ascending curvilinear part which express the mechanical interlocking resistance due to the helical shaped part of the strand. The second stage is characterized by a horizontal plateau which express the excess slippage and strand elongation due to reaching the mechanical interlocking strength (τ_{cs}). The third stage is characterized by an ascending linear part which represent the bulb-shaped anchorage capacity which is named in the adopted model as the "H-anchorage capacity". Finally, the fourth stage represents the sudden splitting concrete failure.

Equations (1) and (2) represent the strand slippage and bond stress values at each loading stage respectively. As illustrated in Eq. (2.b) the bond strength due to the mechanical interlocking resistance τ_{cs} is influenced by the concrete compressive strength and the straight bonded length of the strand. The straight bonded length is equal to the bonded length minus the bulb-shaped length which is estimated to be an average length of 120 mm.

The bond strength of the concrete-strand system with a bulb-shaped dead end anchorage depends on the mechanical interlocking strength and the capacity of the bulb-shaped anchorage, which is referred as the "H-anchorage capacity" in Eq. (2.d). In the next section a verification will be conducted to assess the validity of applying the predicted equations proposed by the adopted bond model to estimate the bond strength of strands with bulb-shaped dead end anchorage in concrete slabs.

$$S_{1s} = 1.91 + 5.4 \times 10^{-3} Ls \tag{1.a}$$

$$S_{2s} = 3.8 + 5.3 \times 10^{-3} Ls \tag{1.b}$$

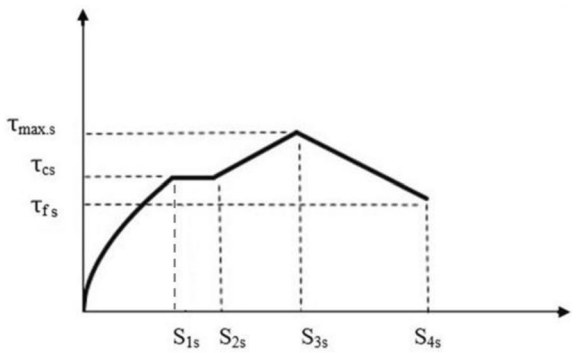

Fig. 10 Bond model of strand with bulb-shaped dead end and concrete (Aly et al., 2023)

$$S_{3s} = 2.55 + 18 \times 10^{-3} Ls \quad (1.c)$$

$$S_{4s} = S3 + 5.91mm \quad (1.d)$$

$$\tau_s = \tau_{cs}(s/s_{1s})^{0.7} \quad \text{for } 0 < S < S_{1s} \quad (2.a)$$

$$\tau_{cs} = (450/L_s)\sqrt{f}_c * (1/L_s)^{0.05} \quad (2.b)$$

$$\tau_S = \tau_{cs} \quad \text{for } S_{1s} < S < S_{2s} \quad (2.c)$$

$$\tau_{max.s} = \tau_{cs} + H\ anchorage\ capacity \quad \text{for } S_{2s} \le S < S_{3s} \quad (2.d)$$

(An approximate average value for H-anchorage capacity = 2 MPa)

$$\tau_s = \tau_{fs} + \left(\tau_{max.s} - \tau_{fs}\right)\frac{S_{4s} - S}{S_{4s} - S_{3s}} \quad \text{for } S_{3s} \le S < S_4 s \quad (2.e)$$

$$\tau_{fs} = \tau_{max.s} - 2.86Mpa \quad (2.f)$$

where

τ_s = Bond stress in (MPa) at slippage (S) in (mm).
τ_{cs} = Mechanical interlocking strength (MPa).
$\tau_{max.s}$ = Maximum bond stress (MPa).
τ_{fs} = bond stress at failure (MPa).
f_c = Average concrete cube compressive strength.
$S_{1s,}$ $S_{2s,}$ S_{3s} and S_{4s} = Characteristic slippage at point 1, 2, 3 and 4 respectively in (mm).
L_s = straight bonded length.

13 Verification of the Adopted Bond Model

In order to validate the use of the adopted bond model for evaluating the bond strength of strand with bulb-shaped dead end anchorage in concrete slab segments. The predicted equations were used to evaluate the bond strength theoretically and Eq. (3) was used to calculate the bond strength experimentally. The experimental bond strength was calculated by dividing the ultimate load (P_u) by the surface area of the straight bonded length of the strand, considering the bulb-shaped dead end anchorage as an anchorage point for simplicity. The strand surface area at the straight bonded length is equal to the perimeter of the circumference wires (1.33 πD) multiplied by the straight bonded length (L_s), where 1.33 is the perimeter expanded coefficient based on the strand cross section properties (Yi et al., 2020b) and D is the strand diameter.

$$\tau_{s(\exp.)} = \frac{P_u}{1.33\pi DL_s} \quad (3)$$

Figs. 11, 12 and 13 shows the comparison between the bond-slip relationships resulted from the experimental pullout tests and the adopted bond model (Aly et al., 2023) for "N", "M" and "H" specimens respectively. It was observed from the relationships obtained from the experimental results that the horizontal plateau which represent the mechanical interlocking strength was absent when applying the proposed equations to the tested slab segments. This could be attributed to the presence of traditional longitudinal reinforcement which helps in resisting the tensile stresses conducted along the specimen length. Consequently, determining the mechanical interlocking strength (τ_c) experimentally becomes challenging.

A comparison between the maximum bond stress calculated experimentally from Eq. (3) and theoretically from Eq. (2.d) is illustrated in Table 4. As observed from Table 4, the experimental τ_{max} exceeds the predicted τ_{max} by 22% for specimen "N" with a concrete compressive strength of 34 MPa. Additionally, the experimental τ_{max} exceeds the predicted τ_{max} by an average of 12.5% and 3% for specimens "M" and "H" with concrete compressive strength of 48 MPa and 70 MPa respectively. This shows that the predicted equation for bond strength underestimate the bond stress between concrete and strand with bulb-shaped dead end anchorage at normal concrete compressive strength and provides a very reasonable value at high strength concrete.

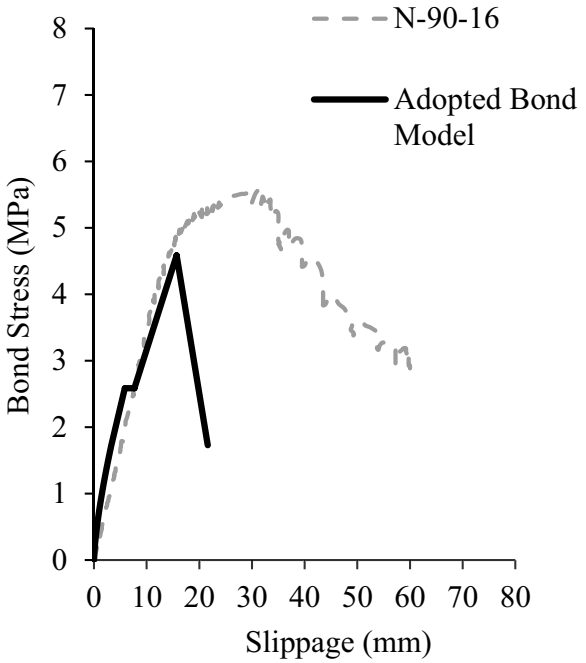

Fig. 11 Comparison between the bond stress-slip relationship of "N" specimen with the adopted bond model

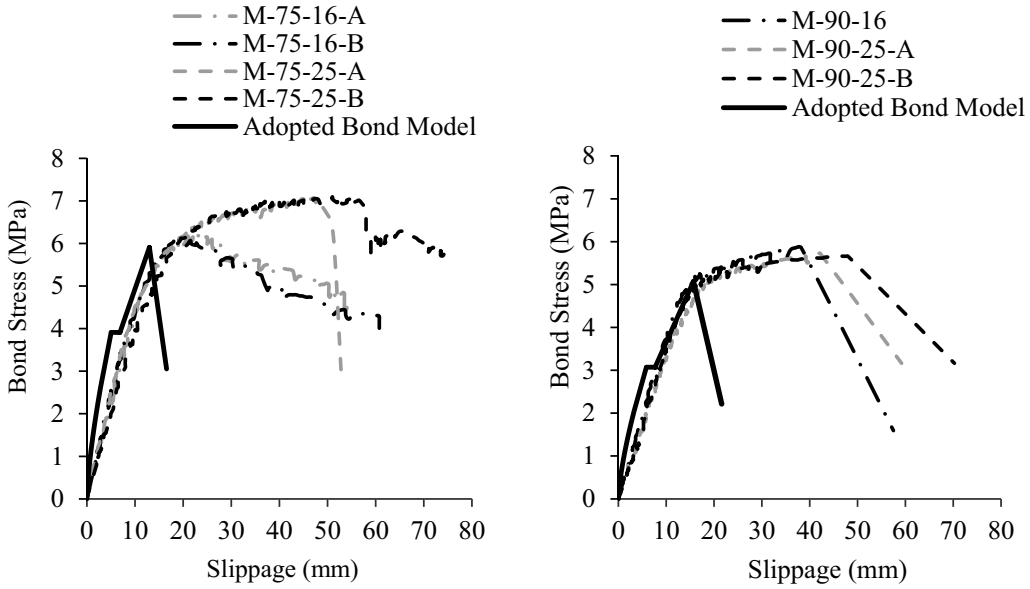

Fig. 12 Comparison between the bond stress-slip relationships of "M" specimens with the adopted bond model

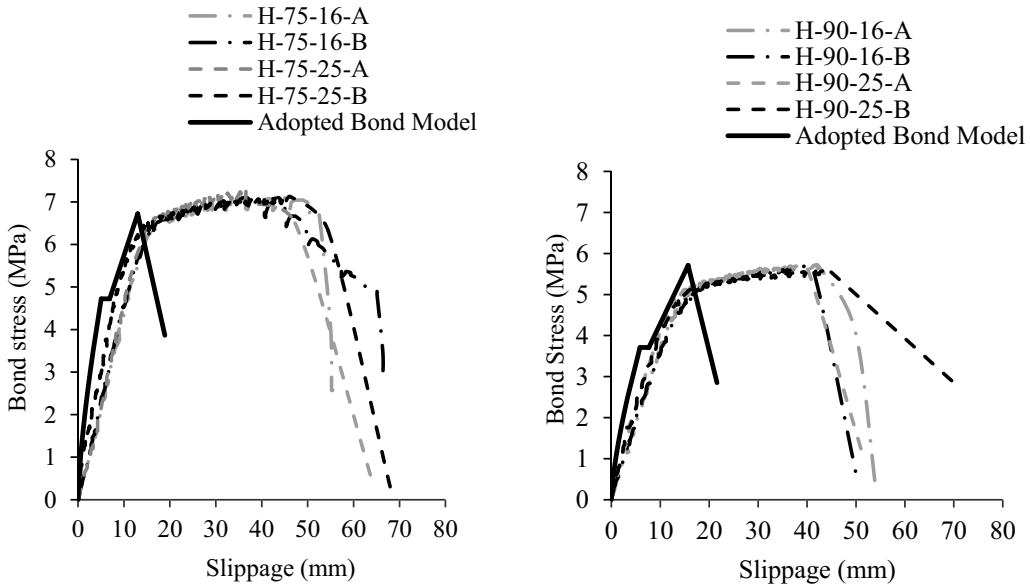

Fig. 13 Comparison between the bond stress-slip relationships of "H" specimens with the adopted bond model

Equation (2.f) which expresses the failure bond stress τ_f could not be useful for application in case of reinforced slab specimens because the transverse reinforcement and stirrups located around the bulb-shaped dead end anchorage provide more ductility as observed in the bond stress-slip relationships shown in Figs. 11, 12. This consequently, reduces the occurrence of sudden splitting failure at the dead end location if compared by the adopted bond model curve.

The adopted bond model could provide a reasonable prediction for bond strength between concrete and strand with bulb-shaped dead end anchorage in slabs based on the concrete compressive strength and the straight bonded length and consequently it could be used to expect the minimum failure load.

Table 4 Comparison between the maximum bond stress values theoretically and experimentally

Specimen Name	P_u (kN)	f_c (MPa)	L_b (mm)	L_S (mm)	τ_{max} experimental	$\tau_{max.s}$ predicted	$\tau_{max.s}$ exp./ $\tau_{max.s}$ pred
M-75-16-A	228	48	700	580	6.18	5.91	1.04
M-75-16-B	226		700	580	6.12	5.91	1.04
M-75-25-A	261		700	580	7.07	5.91	1.20
M-75-25-B	262		700	580	7.10	5.91	1.20
N-90-16	259	34	850	730	5.57	4.59	1.22
M-90-16	272	48	850	730	5.85	5.07	1.15
M-90-25-A	266		850	730	5.73	5.07	1.13
M-90-25-B	263		850	730	5.66	5.07	1.12
H-75-16-A	262	70	700	580	7.10	6.72	1.06
H-75-16-B	263		700	580	7.12	6.72	1.06
H-75-25-A	268		700	580	7.26	6.72	1.08
H-75-25-B	263		700	580	7.12	6.72	1.06
H-90-16-A	266		850	730	5.73	5.71	1.00
H-90-16-B	262		850	730	5.64	5.71	0.99
H-90-25-A	264		850	730	5.68	5.71	1.00
H-90-25-B	260		850	730	5.60	5.71	0.98

14 Conclusion

Indirect pull-out tests were conducted on 15.24 mm diameter prestressing strands with bulb-shaped dead end anchorage embedded inside slab segments. These segments represented the dead end zone of post-tensioning concrete slabs. The purpose was to determine the sufficient development length in slabs of different thicknesses and concrete compressive strengths with minimum strand spacing equal 300 mm. Based on the experimental test results, the following conclusions were driven:

1. At concrete compressive strength equal to 70 MPa, 700 mm bonded length is considered as a safe development length for strand with bulb-shaped dead end anchorage in post-tensioning slabs, as it reaches the strand ultimate strength. Additionally, the same bonded length can develop the strand ultimate strength for slab thickness not less than 250 mm at concrete compressive strength equal to 48 MPa.
2. At different concrete compressive strengths 34 MPa, 48 MPa and 70 MPa, a bonded length of 850 mm with minimum slab thickness 160 mm is a sufficient development length to develop the strand ultimate strength.
3. Increasing the slab thickness significantly decreases the crack propagation as it leads to more concrete confinement around the bulb-shaped dead end anchorage
4. The effect of increasing concrete compressive strength is more significant in decreasing or eliminating concrete cracks due to the increases in the concrete tensile strength.
5. A verification was carried out between a predicted equations conducted from an adopted bond model and the experimental test results of the tested slab segments. The results confirm the validity and the eligibility of using the predicted equations to assess the bond strength of strand with bulb-shaped dead end anchorage in post-tensioning slabs.
6. The adopted bond model could predict a reasonable value for the bond strength between concrete and strand with bulb-shaped dead end anchorage in post-tensioning slabs, based on concrete compressive strength and straight bonded length and it shall also anticipate the minimum failure load.

Acknowledgements
Not applicable.

Author contributions
Jehan H. Aly: Resources, Investigation, Validation, Visualization, Writing—Original Draft. A. Farghal Maree: Conceptualization, Methodology, Validation, Visualization, Review & Editing. Mohamed Kohail: Conceptualization, Methodology, Validation, Visualization, Review and Editing. Ayman H. Khalil: Conceptualization, Methodology, Validation, Visualization, Supervision, Review and Editing.

Funding
Open access funding provided by The Science, Technology & Innovation Funding Authority (STDF) in cooperation with The Egyptian Knowledge Bank (EKB).

Availability of data and materials
All data generated or analyzed during this study are included in this published article.

Declarations

Competing interests
No competing interests exits in the submission of this manuscript, and manuscript is approved by all authors for publication. The author declare that the work described was original research that has not been published previously, and not under consideration for publication elsewhere.

Received: 18 September 2023 Accepted: 8 May 2024
Published: 25 September 2024

References

ACI 318-, *(ACI 318–19) Building Code Requirements for Structural Concrete ,Commentary on Building Code Requirements for Structural Concrete (ACI 318R-19) ACI*. 2019.

"American Society for Testing and Materials.ASTM A1081 / A1081M-15, "Standard Test Method for Evaluating Bond of Seven-Wire Steel Prestressing Strand," 2015. doi: https://doi.org/10.1520/A1081.

Aly, J. H., Farghl Maree, A., Kohail, M., & Khalil, A. H. (2023). Modeling of bond stress-slip relationships of mono-prestressing strands with H-anchorage dead end. *Ain Shams Engineering Journal, 14*(6), 102105. https://doi.org/10.1016/j.asej.2022.102105

Barnes, R. W., Burns, N. H., & Kreger, M. E. (1999). Development length of 0.6-inch prestressing strand in standard I-Shaped pretensioned concrete beams. *University of Texas at Austin Center for Transportation Research, 7*(22), 338.

Buckner, C. D. (1995). A review of strand development length for pretensioned. *PCI Journal, 40*(2), 84–105.

CEB-FIP, "CEB_FIP_model_code_1990_ing.pdf." p. 462, 1990.

Dang, C. N., Floyd, R. W., Hale, W. M., & Martí-Vargas, J. R. (2016). Measured development lengths of 0.7 in. (17.8 mm) strands for pretensioned beams. *ACI Structural Journal, 113*(3), 525–535. https://doi.org/10.14359/51688823

Dang, C. N., Floyd, R. W., Murray, C. D., Hale, W. M., & Martí-Vargas, J. R. (2015b). Bond stress-slip model for 0.6 in. (15.2 mm) diameter strand. *ACI Structural Journal, 112*(5), 625–634. https://doi.org/10.14359/51687750

Dang, C. N., Hale, W. M., Floyd, R. W., & Martí-Vargas, J. R. (2018). Prediction of development length from free-end slip in pretensioned concrete members. *Magazine of Concrete Research, 70*(14), 714–725. https://doi.org/10.1680/jmacr.17.00334

Dang, C. N., Murray, C. D., Floyd, R. W., Hale, W. M., & Martí-Vargas, J. R. (2014a). Correlation of strand surface quality to transfer length. *ACI Structural Journal, 111*(5), 1245–1252. https://doi.org/10.14359/51686925

Dang, C. N., Murray, C. D., Floyd, R. W., Hale, W. M., & Martí-Vargas, J. R. (2014b). Analysis of bond stress distribution for prestressing strand by standard test for strand bond. *Engineering Structures, 72*(August), 152–159. https://doi.org/10.1016/j.engstruct.2014.04.040

Dang, C. N., Murray, C. D., Hale, W. M., Marti-Vargas, J. "A review of factors influencing strand bond," *Pci/Nbc*, no. February 2015, 2013.

Egyptian code of practice ECP 203: design and construction for reinforced concrete structures, ministry of building construction, research center for housing, building and physical planning. 2018.

El Zghayar, E. A. "Transfer and Development Length of Strands in Post-Tensioned Members After Anchor Head Failure," University of Central Florida, 2007.

Fabris, N., Faleschini, F., Zanini, M. A., Pellegrino, C., "Assessment of influencing parameters on transmission length of prestressed concrete," in *Proceedings of the 12th fib International PhD Symposium in Civil Engineering*, 2018, pp. 387–395.

Fabris, N., Faleschini, F., Zanini, M. A., Pellegrino, C. "Assessment of influencing parameters on transmission length of prestressed concrete," *fib Symp.*, no. September, pp. 387–395, 2018.

Farghal Maree, A., & Hilal Riad, K. (2014). Analytical and experimental investigation for bond behaviour of newly developed polystyrene foam particles' lightweight concrete. *Engineering Structures, 58*, 1–11. https://doi.org/10.1016/j.engstruct.2013.10.015

Fédération Internationale du Béton,FIB Model Code, International Federation for Structural Concrete, no. 1. 2013.

Ghosh, S. K., & Fintel, M. (1986). Development length of prestressing strands, including debonded strands, and allowable concrete stresses in pretensioned members. *PCI Journal, 31*(5), 38–57. https://doi.org/10.15554/pcij.09011986.38.57

Hanson, N. W., & Kaar, P. H. (1959). Flexural bond tests of pretensioned prestressed beams. *ACI Journal Proceedings*. https://doi.org/10.14359/11389

Hong, J.-S., Jung, H.-S., Bae, B.-I., Choi, C.-S., "Numerical approach to evaluation of bond strength of headed bars," in *IABSE Congress, Seoul 2012: Innovative Infrastructures – Towards Human Urbanism*, 2012, https://doi.org/10.2749/222137912805112617.

Hong, S., & Park, S. K. (2012). Uniaxial bond stress-slip relationship of reinforcing bars in concrete. *Advances in Materials Science and Engineering*. https://doi.org/10.1155/2012/328570

Janney, J. (1954). Nature of bond in pre-tensioned prestressed concrete. *ACI Journal Proceedings*. https://doi.org/10.14359/11790

Jiang, X., Gui, Q., & Ma, Z. J. (2019). Pretensioned pullout test of 18 mm (0.7 in.) diameter strand with different embedment lengths. *Structural Concrete, 20*(6), 1842–1857. https://doi.org/10.1002/suco.201800215

Kareem, R. S., Al-Mohammedi, A., Dang, C. N., Dang, C. N., Martí-Vargas, J. R., & Hale, W. M. (2020). Bond model of 15·2 mm strand with consideration of concrete creep and shrinkage. *Magazine of Concrete Research, 72*(15), 799–810. https://doi.org/10.1680/jmacr.18.00506

Kobrosli, H., et al. (2022). Influence of various design parameters of the grouted duct on mono-strand bond behavior in post tensioned members. *Journal of Materials Research and Technology, 17*, 1232–1245. https://doi.org/10.1016/j.jmrt.2022.01.034

Lee, C., Shin, S., Lee, S., & Oh, J. (2017). Modeling of bond stress-slip relationships of a strand in concrete during steam curing. *International Journal of Concrete Structures and Materials*. https://doi.org/10.1007/s40069-017-0210-y

Lin, H., Zhao, Y., Ozbolt, J., Feng, P., Jiang, C., & Eligehausen, R. (2019). Analytical model for the bond stress-slip relationship of deformed bars in normal strength concrete. *Construction and Building Materials, 198*, 570–586. https://doi.org/10.1016/J.CONBUILDMAT.2018.11.258

Logan, D. R. (1997). Acceptance criteria for bond quality of strand for pretensioned prestressed concrete applications. *PCI Journal, 42*(2), 52–79. https://doi.org/10.15554/pcij.03011997.52.90

Martí-Vargas, J. R., García-Taengua, E., & Serna, P. (2013). Influence of concrete composition on anchorage bond behavior of prestressing reinforcement. *Construction and Building Materials, 48*, 1156–1164. https://doi.org/10.1016/j.conbuildmat.2013.07.102

Mazumder, M. H., Gilbert, R. I., & Chang, Z. T. (2021). Analytical model for bond–slip behavior of the anchorage of deformed bars in reinforced concrete members subjected to bending. *Journal of Building Pathology and Rehabilitation, 6*(1), 1–11. https://doi.org/10.1007/s41024-021-00126-1

Mitchell, D., Cook, W. D., & Tham, T. (1993). Influence of high strength concrete on transfer and development length of pretensioning strand. *PCI Journal*. https://doi.org/10.15554/pcij.05011993.52.66

Mohammedali, T. K., Abdullah, K. S., Mohammed, A. H., Khalaf, R. D., & Hussin, A. K. (2021). A review of studies on the post-tensioned concrete beams. *AIP Conference Proceedings*. https://doi.org/10.1063/5.0068963

Mohandoss, P., Pillai, R. G., & Gettu, R. (2021). Determining bond strength of seven-wire strands in prestressed concrete. *Structures, 33*, 2413–2423. https://doi.org/10.1016/j.istruc.2021.06.004

Mohandoss, P., Pillai, R. G., & Sengupta, A. K. (2020). Effect of compressive strength of concrete on transmission length of pre-tensioned concrete systems. *Structures, 23*(December), 304–313. https://doi.org/10.1016/j.istruc.2019.09.016

Mohandoss, P., Pillai, R. G., & Sengupta, A. K. (2020b). Effect of compressive strength of concrete on transmission length of pre-tensioned concrete systems. *Structures, 23*, 304–313. https://doi.org/10.1016/j.istruc.2019.09.016

Naito, C., Cetisli, F., & Tate, T. (2015). A method for quality assurance of seven-wire strand bond in portland cement concrete. *PCI Journal, 60*(4), 69–84. https://doi.org/10.15554/pcij.07012015.69.84

Nawy, E. G. (2009). *Reinforced concrete: a fundamental approach*. New Jersey: Pearson.
Oh, B. H., & Kim, E. S. (2000). Realistic evaluation of transfer lengths in pretensioned prestressed concrete members. *ACI Structural Journal, 97*(6), 821–830.
Osama, R. A. A.-H. M. R. "Study the failure of post-tension slab in multy-story building in eastern area , KSA .," 2009.
Peterman, R. (2009). A simple quality assurance test for strand bond. *PCI Journal*. https://doi.org/10.15554/pcij.03012009.143.161
P. Rogowsky, D M - Marti, "Detailing for Post-Tensioned," Switzerland, 1991. www.vsl.com.
Salmons, J. R., & McCrate, T. E. (1977). Bond characteristics of untensioned prestressing strand. *PCI Journal, 22*(1), 52–65. https://doi.org/10.15554/pcij.01011977.52.65
Shin, H. O., Lee, S. J., & Yoo, D. Y. (2018). Bond behavior of pretensioned strand embedded in ultra-high-performance fiber-reinforced concrete. *International Journal of Concrete Structures and Materials*. https://doi.org/10.1186/s40069-018-0249-4
Sofi, M., Mendis, P., Baweja, D., & Mak, S. (2014). Influence of ambient temperature on early age concrete behaviour of anchorage zones. *Construction and Building Materials, 53*(November), 1–12. https://doi.org/10.1016/j.conbuildmat.2013.11.051
Sorensen,A. D., Hill O. M., and Ut L., "Bond Performance of 1–1 / 8 Inch Diameter Prestressing Strands Bond Performance of 1–1 / 8 Inch Diameter Prestressing Strands Submitted by," 2019. doi: https://doi.org/10.13140/RG.2.2.30099.84003.
Tang, C. W. (2015). Local bond stress-slip behavior of reinforcing bars embedded in lightweight aggregate concrete. *Computers and Concrete, 16*(3), 449–466. https://doi.org/10.12989/cac.2015.16.3.449
Tang, C. W. (2017). Uniaxial bond stress-slip behavior of reinforcing bars embedded in lightweight aggregate concrete. *Structural Engineering and Mechanics, 62*(5), 651–661. https://doi.org/10.12989/sem.2017.62.5.651
Tang, C. W., & Cheng, C. K. (2020). Modeling local bond stress-slip relationships of reinforcing bars embedded in concrete with different strengths. *Materials*. https://doi.org/10.3390/MA13173701
Transfer, Development, and Splice Length for Strand/Reinforcement in High-Strength Concrete," *Transf. Dev. Splice Length Strand/Reinforcement High-Strength Concr.*, 2008, doi: https://doi.org/10.17226/13916.
Wang, L., Yuan, P., Xu, G., & Han, Y. (2022). Quantification of non-uniform mechanical interlock and rotation in modelling bond-slip between strand and concrete. *Structures, 37*, 403–410. https://doi.org/10.1016/j.istruc.2022.01.024
Wang, L., Zhang, X., Zhang, J., Yi, J., & Liu, Y. (2017). Simplified model for corrosion-induced bond degradation between steel strand and concrete. *Journal of Materials in Civil Engineering*. https://doi.org/10.1061/(asce)mt.1943-5533.0001784
Yang, J. M., Kim, J. K., & Yoo, D. Y. (2018). Transfer length in full-scale pretensioned concrete beams with 1.4 m and 2.4 m section depths. *Engineering Structures, 171*, 433–444. https://doi.org/10.1016/j.engstruct.2018.05.104
Yang, R., Yang, Y., Zhang, X., & Wang, X. (2022). Experimental study on performance of local bond-slip test of steel strand tendons and concrete. *Coatings, 12*(10), 1–13. https://doi.org/10.3390/coatings12101494
Yi, J., Wang, L., & Floyd, R. W. (2020b). Bond strength model of strand in corrosion-induced cracking concrete. *ACI Structural Journal, 117*(6), 119–132. https://doi.org/10.14359/51728060
Yi, J., Wang, L., Floyd, R. W., & Zhang, J. (2020a). Rotation-affected bond strength model between steel strand and concrete. *Engineering Structures*. https://doi.org/10.1016/j.engstruct.2019.110060
Yu, T., Xue, P. "Utilizing plastic deformation for energy absorption," in *Introduction to Engineering Plasticity*, Elsevier, 2022, pp. 293–326.

Publisher's Note

Jehan H. Aly PhD Candidate, Structural Engineering Department, Faculty of Engineering, Ain Shams University, Egypt.

A. Farghal Maree Assistant Professor, Structural Engineering Department, Faculty of Engineering, Ain Shams University, Egypt.

Mohamed Kohail Associate Professor, Structural Engineering Department, Faculty of Engineering, Ain Shams University, Egypt.

Ayman H. Khalil Professor of Concrete Structures, Structural Engineering Department, Faculty of Engineering, Ain Shams University, Egypt.